The formation of an energy gap in graphene on ruthenium by controlling the interface

The formation of an energy gap in graphene on ruthenium by controlling the interface

C Enderlein[1,2,3]**, Y S Kim**[1]**, A Bostwick**[1]**, E Rotenberg**[1]
and K Horn[2]

[1] Advanced Light Source, Lawrence Berkeley National Laboratory, Berkeley, CA, USA
[2] Fritz-Haber-Institut der Max-Planck-Gesellschaft, Berlin, Germany
E-mail: carsten@fhi-berlin.mpg.de

Abstract. In this work, we have investigated the spectral function of graphene on a monolayer of intercalated gold on Ru(0001) using angle-resolved photoemission spectroscopy (ARPES). The intercalation leads to a decoupling of the graphene film, as documented by emergence of the characteristic linear π-bands near the Fermi level. However, a band gap at the band crossing is observed. We relate this gap opening to the broken symmetry of the two carbon sublattices, induced by the special lattice mismatch of the graphene and the intercalated gold monolayer.

Contents

1. Introduction

Since its first preparation by exfoliation [1, 2], graphene has become one of the most discussed topics in materials science. Its unusual properties, e.g. an extremely high mobility of charge

---

[3] Author to whom any correspondence should be addressed.

carriers [3, 4] and the quantum Hall effect observed at room temperature [5], render graphene a promising candidate for future electronic devices [6]. These properties derive from the equivalence of the quasi-particles to massless Dirac fermions and the conical shape of the π- and π^*-bands that cross only at two points (K and K′) of the Brillouin zone.

The lack of an energy gap near these crossings (at the Dirac energy E_D) limits the potential applications of graphene, and preparing graphene-based systems with a gap is an important step towards future graphene engineering. The simplest mechanism for opening a gap is by breaking the symmetry of the two graphene sublattices that protect this gap [7], for example in armchair nanoribbons [8] and in biased graphene bilayers [9, 10], or by breaking the sublattice symmetry by bonding graphene (or bilayer graphene) to a substrate [11].

Epitaxial graphene on SiC(0001) presents an anomalous bandstructure near E_D, which has been interpreted as being due to either many-body renormalization (i.e. 'kinking') of the bands caused by electron–plasmon scattering [12]–[18], or to symmetry breaking caused by substrate bonding as outlined above [19, 20]. These behaviors are distinguished by the presence or absence of an energy gap, though interpretation of the data has been controversial [21, 22]. A gap-like spectrum in disordered graphene has recently been demonstrated [23], so it is important when comparing samples that the number of defects be minimized in order to observe the intrinsic spectral function.

Here, we show that in a single system—graphene grown on the Ru(0001) surface—the behavior of the graphene bands near E_D can be selected between two extremes, (i) exhibiting specific many-body kinks and (ii) a situation where a gap appears, by controlling the structure of the graphene–Ru interface. When the first layer below graphene is a graphene-like 'buffer layer', the spectrum is kinked because of many-body interactions, but when this buffer layer is replaced with a layer of Au atoms, the spectrum changes to an unmistakably gapped one. This is the first direct observation of a gap at the Dirac point in a sample without the complications of small domain size or high defect density [21, 22].

2. Experimental details

The angle-resolved photoemission spectroscopy (ARPES) experiments were performed at the Electronic Structure Factory at Beamline 7 of the Advanced Light Source of Lawrence Berkeley National Laboratory by using a photon energy of 95 eV. The photoemission intensity data sets over the energy–momentum space (E, k_x, k_y) were collected with a Scienta R4000 energy analyzer with samples on a liquid He-cooled, three-axis goniometer at $T = 20$ K. The energy/momentum resolutions were 30 meV 0.01 Å^{-1}. The base pressure during measurements was $< 7 \times 10^{-11}$ mbar.

Graphene on Ru was prepared using the carbon segregation method [24, 25]. Sample preparation was performed in an attached chamber with a base pressure of 1×10^{-10} mbar and then characterized by low-energy electron diffraction (LEED). The (0001) surface of the Ru crystal was cleaned by alternately exposing the sample to oxygen (10^{-8} mbar) and ultrahigh vacuum conditions at 1300 °C. The segregation was performed via a slow-cooling process of the Ru crystal from 1000 °C down to room temperature. Depending on the cooling rate, one or two layers of graphene on Ru(0001) could be grown.

Recent studies demonstrate the high quality of such graphene overlayers [24, 26]. The initial graphene layer on the Ru(0001) surface exhibits a hexagonal superstructure with a periodicity of 30 Å [31], which was attributed to the lattice mismatch of about 10% between
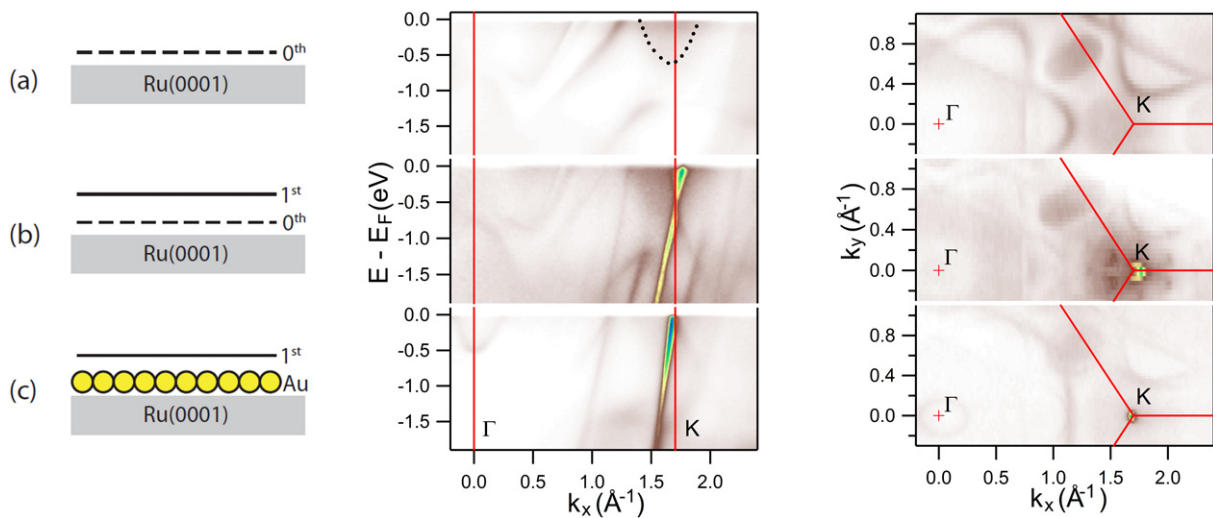
Figure 1. Simplified schematics (left column) and photoemission intensity maps of the bands along the $\Gamma-K$ direction of the hexagonal Brillouin zone (middle column) and constant energy photoemission maps at the Fermi level (right column) of (a) the buffer layer, (b) the buffer and the first graphene layer and (c) a graphene layer formed by intercalation of gold between the former buffer layer, leading to transformation of the buffer into a graphene layer.

graphene (lattice constant $a = 2.46\,\text{Å}$) and the Ru(0001) substrate ($a = 2.706\,\text{Å}$) [27]. *Ab initio* calculations suggest that this mismatch is accommodated by a pronounced rippling, resulting in a position-dependent strength of interaction with the substrate [28, 29], but experiments show partially contradictory results [24, 26]. The initial graphene layer, while metallic, does not show a clear π-band crossing at E_F [30], whereas the subsequent one and two layers show mono- and bilayer graphene-like bandstructures [25], respectively. We therefore call the initial layer the buffer layer (in analogy with the situation on SiC(0001)) and subsequent layers the first, second, etc graphene layers.

Gold intercalation under graphene was accomplished by depositing a thick Au film (>3 ML) on top of the buffer layer, followed by light annealing, after which most of the gold evaporates, leaving a single layer intercalated underneath the buffer layer. As can be seen in figure 1, the buffer layer is transformed into a true graphene layer with sharp π-bands and a clear Fermi surface. That the remaining gold is underneath and not on top is obvious from the lack of attenuation of the resulting graphene ARPES signal.

3. Results and discussions

Figure 1 compares the bandstructures and Fermi surfaces of three different graphene overlayer systems: (a) the buffer layer on Ru(0001), (b) a graphene layer (on top of the buffer) and (c) a graphene layer on top of Au/Ru(0001), decoupled from the Ru substrate by gold intercalation. The spectral function of the buffer layer is characterized by the absence of well-ordered structure of the graphene π-bands in the vicinity of the Fermi level, in agreement with a previous study [30] that shows that the Dirac energy E_D in the buffer layer on Ru is shifted by 2.6 eV

to higher binding energies (BEs) compared to those for pure graphite. This can be attributed to the strong interaction between this layer and the ruthenium substrate, leading to a strong hybridization between graphene π and Ru 4d valence band states [28].

Such interaction leads to the formation of an unusual 'cloudy' structure around the K-point (shown by the dashed line in figure 1(a)) [30]. Although the interpretation of this cloudy feature as an energy band is not straightforward (since it is not predicted by DFT calculations [30]), we can take its general shape to indicate an electron pocket derived from the graphene π-band, but heavily modified by strong interactions of the graphene monolayer on ruthenium, and inhomogeneously broadened due to the spatially varying interaction strength.

The formation of the first graphene monolayer (on top of the buffer layer) on Ru(0001) leads to dramatic changes in the electronic structure of the system. We now observe a linearly dispersing π-band around the K-point that crosses the Fermi level, reflecting the massless behavior of electron carriers in the graphene layer. There is no apparent interaction between the bands in the two layers. The graphene layer, however, is n-doped with the position of the Dirac energy E_D at 0.5 eV BE below the Fermi level E_F. We conclude that both layers are doped by charge transfer from the substrate, but only the upper layer's bands strongly resemble pure graphene [25].

Previous studies of graphene on Ni(111) [31, 32] show that upon intercalation with noble metals, the π-states in graphene recover nearly the same bandstructure as pure graphene, showing the linear dispersion of the π-bands in the vicinity of the Fermi level. This reflects the weakening of the interaction between the graphene layer and the substrate. Figure 1(c) shows the electronic structure as well as a photoemission intensity map at the Fermi level of the 1 ML graphene/Au/Ru(0001) system. Now, the buffer layer is transformed into a true graphene layer with sharp π-bands and a clear Fermi surface. That the remaining gold is underneath and not on top is obvious from the lack of attenuation of the resulting graphene ARPES signal. We estimate, based on core-level intensity measurements (not shown in this paper), that the Au layer thickness is about 1 ML, independent of the pre-deposited Au layer thickness. The same thickness of intercalated gold was obtained for the graphene/Au/Ni(111) system [33]. The spectral function around the Γ-point still reveals weak photoemission intensity from the gold surface state, indicating residual gold islands on top of the graphene system [33].

The intercalation of Au underneath 1 ML of graphene on Ru(0001) leads to an energy shift of the π-band of the graphene layer to lower BEs compared to both single-layer and bilayer graphene on Ru(0001). This demonstrates the weakness of the interaction between the single graphene layer and the gold layer. The Fermi surface appears to be pointlike in figure 1(c); however, a close look at the dispersion of the π-states around the Fermi level (figure 2 (left side, lower panel)) reveals that the Dirac point is ~150 meV above E_F, consistent with a small p-doping of the graphene layer in the 1 ML graphene/Au/Ru(0001) system. A similar p-doping of graphene was recently observed in the case of deposition and annealing of a thin gold layer on the graphene monolayer on SiC(0001) [34].

In order to study the shape of the bands around E_D, it is necessary to push the band crossing below the Fermi level by n-type doping. This was done by controlled deposition of potassium atoms on top of the 1 ML graphene/Au/Ru(0001) system [10], upon which the π-band and the Dirac point shift rigidly to higher BEs with increasing K dosage. Surprisingly, with increasing doping a clear energy gap for π-states becomes visible at E_D (figure 2). Comparison of graphene layers on ruthenium bandstructures recorded at high energy and angular momentum resolution as a function of the interface composition is shown in figure 3. From the conical shape of the
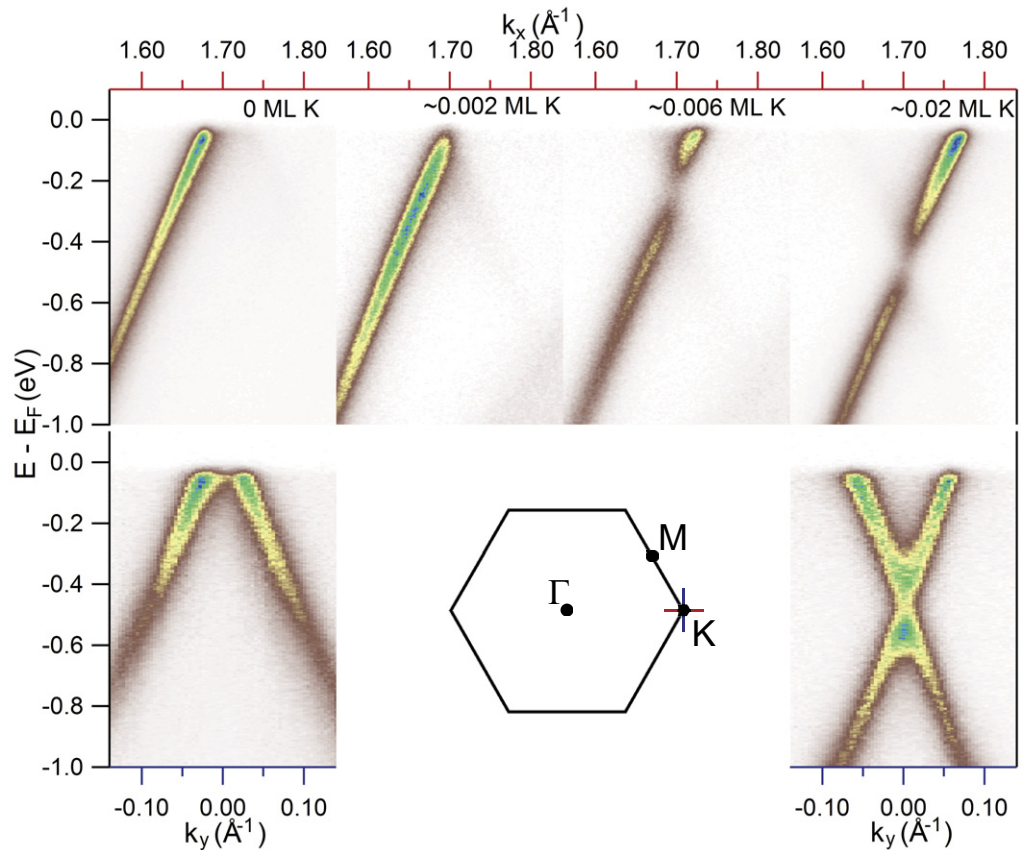
Figure 2. A series of photoemission intensity maps around the K-point of the Brillouin zone of the 1 ML graphene/Au/Ru(0001) system for clean (left column) and progressive doping with potassium. The upper and lower rows are taken along the two orthogonal directions in the reciprocal space as indicated by the red and black lines at the K-point in the Brillouin zone (inset).

π^*-bands, the K-point spectrum (and hence the Dirac crossing energies E_D) can be unambiguously determined. For the graphene/buffer layer system (figure 3(a)), we find that, within the limits of our experimental resolution, which account for 30 meV, the bandstructure at K exhibits no gap. Instead, it exhibits the appearance of a weak kink around E_D, consistent with the influence of electron–plasmon coupling as reported for graphene on SiC [12, 35] and predicted for free-standing graphene [15, 16, 18]. The energy distribution curve (EDC) at the K-point (see the right panel of figure 3(a)) can be represented by a single Voigt peak with a full-width at half-maximum (FWHM) of 100 meV. By contrast, n-doped graphene on Au on Ru shows the clear formation of an energy gap at E_D; an analysis of the EDC at the K-point shows that it requires two peaks (of FWHM 100 meV) to model the data, demonstrating that the bandstructure of this graphene layer exhibits a gap of about 200 ± 60 meV. Since we acquired the spectra in figure 3 by a fine sampling of the entire two-dimensional momentum range, we can be sure that the presented bandstructure cuts passed precisely through the K-points and therefore the observed gaps cannot be due to sample misalignment.

A mechanism of gap opening at the K-point due to hybridization with gold states can be excluded, since there are no gold states near E_D. Moreover, a gap opening due to the
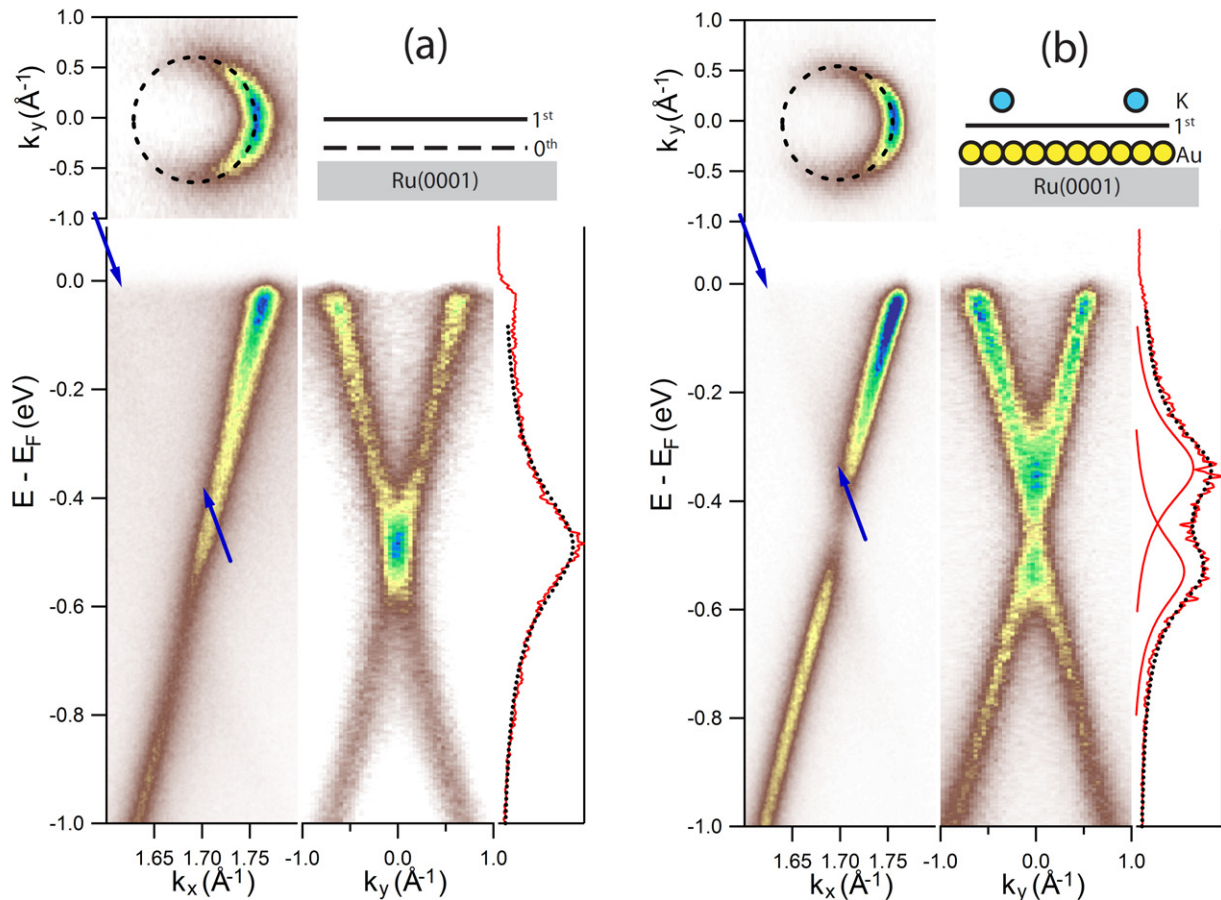
Figure 3. Comparison of the spectral function of 1 ML graphene on (a) the buffer layer or (b) 1 ML gold atoms on Ru(0001). Three cuts of the spectral function are shown along (upper left) the Fermi surface versus (k_x, k_y) and (lower left, right) the bandstructure along the two orthogonal cuts indicated in the inset of figure 2. For both systems the photoemission intensity along the K-point is plotted and fitted with one Voigt peak for the buffer + first and with two Voigt peaks for the Au + first graphene layers on Ru(0001).

formation of a superstructure, as reported by Pivetta *et al* [36], can be excluded, since such a superstructure can easily be determined in our data sets via a sudden change in the bandstructure. Our measurements begin to show such a phase transition with higher potassium coverage. Finally, the band gap does not increase with higher potassium coverage, proving that the potassium is not the reason for the gap opening. Thus, we propose that the band gap in the 1 ML graphene/Au/Ru(0001) system results from a symmetry breaking of the two carbon sublattices in the graphene layer, which results in a weak breaking of the chiral symmetry, inducing a weak but finite intensity of the left band along the Γ–K direction, between the two arrows in figure 3(b) [13, 37, 38]. The ratio of the left to right band intensities in figure 3(b) is about 35, which agrees with theoretical predictions for the size of a gap of 200 meV [13]. Within our statistics, there is no equivalent observable intensity for the graphene/buffer layer/Ru system (between the arrows in figure 3(a)), consistent with the lack of a gap at E_D.

IOP Institute of Physics Φ DEUTSCHE PHYSIKALISCHE GESELLSCHAFT

The appearance of the gap in gold-intercalated graphene is surprising. Calculations [11] indicate a weak bond between noble metals and graphene without a notable gap. While a detailed explanation of why gold intercalation opens a gap will depend on the exact microscopic structure of the interface, which is outside the scope of the present work, we can speculate that the incommensuration between graphene and Au lattice constants (2.46 and 2.81, respectively), neglected in the calculations [11], plays a role. Depending on the exact length scales, the K and K′ points of the graphene can be coupled, amounting to a breaking of the sublattice symmetry in real space that protects the Dirac point from opening a gap. But on the other hand, the strength of the photoemission satellite bands is greatly reduced for interfacial Au compared to the buffer layer, consistent with a related weak potential associated with the Au incommensuration. Therefore, we also see that the band gap results from a symmetry breaking of the two sublattices and is induced by the gold layer; a consistent explanation for the appearance of the gap in the Au case remains elusive. Local probes could help us to solve this issue.

Our results show that intercalation of gold under graphene can be a useful technique to restore graphene's unique properties when its bonding to a substrate strongly modifies its electronic properties. These changes can range from the modest, such as changing the natural doping of the graphene–substrate system, to the more drastic, as in the case where the unique properties of the graphene are lost due to strong substrate hybridization, as with the buffer layer on Ru(0001). Here no symmetry breaking can be observed, consistent with the fact that the buffer layer has the structure of graphene, but the strong bonding to the substrate kills the conical bands [24]. This is a particularly important consideration for the interface between graphene and contacts, either electronic or magnetic.

In conclusion, the electronic structure modification of a single graphene layer on Ru(0001) upon gold intercalation was studied by means of angle-resolved photoelectron spectroscopy. The spectral functions of the bilayer graphene film on Ru(0001) is characterized by the absence of any energy gap in the electronic structure. Surprisingly, the energy gap for the π-states is found after intercalation of Au monolayer underneath graphene monolayer on Ru. The appearance of such a gap in the electronic structure is assigned to the fact that the symmetry for two carbon sublattices is broken in the graphene/Au/Ru(0001) system due to the geometry of the system.

References

[1] Novoselov K S, McCann E, Morosov S V, Fal'ko V I, Katsnelson M I, Zeitler U, Jiang D, Schedin F and Geim A K 2005 Two-dimensional gas of massless Dirac fermions in graphene *Nature* **438** 192–200
[2] Zhang Y, Tan Y W, Stormer H L and Kim P 2005 Experimental observation of the quantum Hall effect and Berry's phase in graphene *Nature* **438** 201–4
[3] Bolotin K I, Sikes K J, Jiang Z, Klima M, Fudenberg G, Hone J, Kim P and Stormer H L 2008 Ultrahigh electron mobility in suspended graphene *Solid State Commun.* **146** 351–5

[4] Du X, Skachko I, Barker A and Andrei E Y 2008 Approaching ballistic transport in suspended graphene *Nat. Nano.* **3** 491–5

[5] Novoselov K S, Jiang Z, Zhang Y, Morozov S V, Stormer H L, Zeitler U, Maan J C, Boebinger G S, Kim P and Geim A K 2007 Room-temperature quantum Hall effect in graphene *Science* **315** 1137201

[6] Geim A K and Novoselov K S 2007 The rise of graphene *Nat. Mater.* **6** 183–91

[7] Jones H 1934 Applications of the Bloch theory to the study of alloys and of the properties of bismuth *Proc. R. Soc.* A **147** 396–417

[8] Nakada K, Fujita M, Dresselhaus G and Dresselhaus M S 1996 Edge state in graphene ribbons: nanometer size effect and edge shape dependence *Phys. Rev.* B **54** 17954

[9] McCann E and Fal'ko V I 2006 Landau-level degeneracy and quantum hall effect in a graphite bilayer *Phys. Rev. Lett.* **96** 086805

[10] Ohta T, Bostwick A, Seyller T, Horn K and Rotenberg E 2006 Controlling the electronic structure of bilayer graphene *Science* **313** 951–4

[11] Giovannetti G, Khomyakov P A, Brocks G, Karpan V M, van den Brink J and Kelly P J 2008 Doping graphene with metal contacts *Phys. Rev. Lett.* **101** 026803–4

[12] Bostwick A, Ohta T, Seyller T, Horn K and Rotenberg E 2007 Quasiparticle dynamics in graphene *Nat. Phys.* **3** 36–40

[13] Bostwick A, Ohta T, McChesney J L, Emtsev K V, Seyller T, Horn K and Rotenberg E 2007 Symmetry breaking in few layer graphene films *New J. Phys.* **9** 385

[14] Hwang E H, Yu-Kuang Hu B and Das Sarma S 2007 Inelastic carrier lifetime in graphene *Phys. Rev.* B **76** 115434

[15] Polini M, Asgari R, Borghi G, Barlas Y, Pereg-Barnea T and MacDonald A H 2008 Plasmons and the spectral function of graphene *Phys. Rev.* B **77** 081411–4

[16] Hwang E H and Das Sarma S 2008 Quasiparticle spectral function in doped graphene: electron–electron interaction effects in ARPES *Phys. Rev.* B **77** 081412–4

[17] Park C-H, Giustino F, Spataru C D, Cohen M L and Louie S G 2009 First-principles study of electron linewidths in graphene *Phys. Rev. Lett.* **102** 076803–4

[18] Park C-H, Giustino F, Spataru C D, Cohen M L and Louie S G 2009 Angle-resolved photoemission spectra of graphene from first-principles calculations *Nano Lett.* **9** 4234–9

[19] Zhou S Y, Gweon G H, Fedorov A V, First P N, de Heer W A, Lee D H, Guinea F, Castro Neto A H and Lanzara A 2007 Substrate-induced bandgap opening in epitaxial graphene *Nat. Mater.* **6** 770–5

[20] Kim S, Ihm J, Choi H J and Son Y-W 2008 Origin of anomalous electronic structures of epitaxial graphene on silicon carbide *Phys. Rev. Lett.* **100** 176802–4

[21] Rotenberg E, Bostwick A, Ohta T, McChesney J L, Seyller T and Horn K 2008 Origin of the energy bandgap in epitaxial graphene *Nat. Mater.* **7** 258–9

[22] Zhou S Y, Siegel D A, Federov A V, El Gabaly F, Schmid A K, Castro Neto A H, Lee D H and Lanzara A 2008 Origin of the energy bandgap in epitaxial graphene *Nat. Mater.* **7** 259

[23] Bostwick A, McChesney J L, Emtsev K V, Seyller T, Horn K, Kevan S D and Rotenberg E 2009 Quasiparticle transformation during a metal insulator transition in graphene *Phys. Rev. Lett.* **103** 056404

[24] Sutter P W, Flege J-I and Sutter E A 2008 Epitaxial graphene on ruthenium *Nat. Mater.* **7** 406–11

[25] Sutter P, Hybertsen M S, Sadowski J T and Sutter E 2009 Electronic structure of few-layer epitaxial graphene on Ru(0001) *Nano. Lett.* **9** 2654–60

[26] Vazquez de Parga A L, Calleja F, Borca B, Passeggi M C G Jr, Hinarejos J J, Guinea F and Miranda R 2008 Periodically rippled graphene: growth and spatially resolved electronic structure *Phys. Rev. Lett.* **100** 056807–4

[27] Martoccia D *et al* Graphene on Ru(0001): a 25 × 25 supercell *Phys. Rev. Lett.* **101** 126102–4

[28] Wang B, Bocquet M-L, Marchini S, Gnther S and Wintterlin J 2008 Chemical origin of a graphene Moir overlayer on Ru(0001) *Phys. Chem. Chem. Phys.* **10** 3530–4

[29] Jiang D-E, Du M-H and Dai S 2009 First principles study of the graphene/Ru(0001) interface *J. Chem. Phys.* **130** 074705–5

[30] Brugger T, Gunther S, Wang B, Hugo Dil J, Bocquet M-L, Osterwalder J, Wintterlin J and Greber T 2009 Comparison of electronic structure and template function of single-layer graphene and a hexagonal boron nitride nanomesh on ru(0001) *Phys. Rev.* B **79** 045407–6

[31] Yu Dedkov S, Shikin A M, Adamchuk V K, Molodtsov S L, Laubschat C, Bauer A and Kaindl G 2001 Intercalation of copper underneath a monolayer of graphite on Ni(111) *Phys. Rev.* B **64** 035405

[32] Varykhalov A, Sanchez-Barriga J, Shikin A M, Biswas C, Vescovo E, Rybkin A, Marchenko D and Rader O 2008 Electronic and magnetic properties of quasifreestanding graphene on Ni *Phys. Rev. Lett.* **101** 157601–4

[33] Shikin A M, Prudnikova G V, Adamchuk V K, Moresco F and Rieder K H 2000 Surface intercalation of gold underneath a graphite monolayer on Ni(111) studied by angle-resolved photoemission and high-resolution electron-energy-loss spectroscopy *Phys. Rev.* B **62** 13202

[34] Gierz I, Riedl C, Starke U, Ast C R and Kern K 2008 Atomic hole doping of graphene *Nano Lett.* **8** 4603–7

[35] Bostwick A, Ohta T, McChesney J L, Seyller T, Horn K and Rotenberg E 2007 Renormalization of graphene bands by many-body interactions *Solid State Commun.* **143** 63–71

[36] Pivetta M, Patthey F, Barke I, Hovel H, Delley B and Schneider W-D 2005 Gap opening in the surface electronic structure of graphite induced by adsorption of alkali atoms: photoemission experiments and density functional calculations *Phys. Rev.* B **71** 165430–4

[37] Shirley E L, Terminello L J, Santoni A and Himpsel F J 1995 Brillouin-zone-selection effects in graphite photoelectron angular distributions *Phys. Rev.* B **51** 13614–22

[38] Mucha-Kruczynski M, Tsyplyatyev O, Grishin A, McCann E, Fal'ko V I, Bostwick A and Rotenberg E 2008 Characterization of graphene through anisotropy of constant-energy maps in angle-resolved photoemission *Phys. Rev.* B **77** 195403